SUPPORTING INFORMATION

Structural Diversity of Arthropod Biophotonic Nanostructures Spans Amphiphilic Phase-Space

Vinodkumar Saranathan,[*,†,‡,⊥,¶] *Ainsley E. Seago,*[§] *Alec Sandy,*[||] *Suresh Narayanan,*[||] *Simon G. J. Mochrie,*[#,¶] *Eric R. Dufresne,*[#,▽,○,¶] *Hui Cao,*[#,▽,¶] *Chinedum O. Osuji,*[◆,¶] *and Richard O. Prum,*[*,⊥,¶]

[†]Division of Physics and Applied Physics, School of Physical and Mathematical Sciences, Nanyang Technological University, 21 Nanyang Link, 637371, Singapore

[‡]Edward Grey Institute of Field Ornithology, Department of Zoology, University of Oxford, South Parks Road, Oxford, OX1 3PS, United Kingdom

[§]CSIRO Ecosystem Sciences, GPO Box 1700, Canberra, Australian Capital Territory 2601, Australia

[||]Advanced Photon Source, Argonne National Laboratory, Argonne, IL 60439, United States

[⊥]Department of Ecology and Evolutionary Biology, and Peabody Museum of Natural History, [#]Department of Physics, [▽]Department of Applied Physics, [○]Department of Mechanical Engineering and Materials Science, [◆]Department of Chemical and Environmental Engineering, and [¶]Center for Research on Interface Structures and Phenomenon (CRISP), Yale University, New Haven, CT 06520, United States

Corresponding authors:
*E-mail: Vinodkumar.Saranathan@aya.yale.edu.
*E-mail: Richard.Prum@yale.edu.

Present Address:
(V.S.) Life Sciences, Yale-NUS College, 6 College Avenue East, 138614, Singapore

(A.E.S.) Agricultural Scientific Collections Unit, NSW Department of Primary Industries, Orange Agricultural Institute, 1447 Forest Road, Orange NSW 2800, Australia

SUPPORTING DISCUSSION

Biological lipids exhibit a propensity to form *inverse* (water-in-oil) or *type-II* phases, where the hydrophilic lipid head-groups curve inward towards the aqueous phase to enclose aqueous cores, producing interfacial curvature termed "negative", by convention[1].

Detailed structural diagnoses of arthropod cuticular photonic nanostructures

In the following, we provide the SAXS and EM structural diagnoses of scale and setae nanostructures organized taxonomically, because different lineages of arthropods appear to have evolved distinct classes of biophotonic nanostructure.

Scales from 19 out of the 127 taxa assayed possessed no obvious coherently scattering nanostructure, as evidenced by the lack of any significant deviations of the corresponding azimuthal scattering profiles from Porod's Law, ruling out any contribution of constructive interference to their observed colors (Figure S1, and Table S1). Porod's Law ($I(q) \propto q^{-4}$) is the 'null' expectation for the scattering from an unstructured material characterized by sharp interfaces or edges separating two media[2, 3]. Nevertheless, the following 8 taxa – *Cyphochilus* sp. (Scarabaeidae), *Urodontus* sp., *Bruchela* sp., *Aonychus* sp., *Nemonyx* sp., *Steriphus* sp., an unknown Cerambycid beetle and *Attus* sp. – exhibited a slight dip in the scattering at low q (< 0.04 nm^{-1}), perhaps suggesting the presence of a highly disordered nanoporous nanostructure that may enhance the background incoherent scattering as in *Cyphochilus* spp.[4, 5] (Figure S1; *cf*. the rudimentary or weakly nanostructured feather barbs in ref. 6). This could also explain the hint of chromaticity in many of these otherwise pale, off-white scales.

The SAXS diffraction patterns from the rest of the 108 taxa assayed consisted either of a number of discrete, high intensity spots arranged in concentric circles (Figures 1m-o, q, and S1)

or a series of concentric, powder-like (or Debye-Scherrer) diffraction rings (Figures 1p, r, and S1), respectively indicating that the associated nanostructures are crystal-like with long-range periodicity or quasi-ordered (amorphous) with short-range isotropic order[7, 8]. The diffraction patterns with a polycrystalline texture (a large number of concentric spots), indicates the presence of multiple domains with dimensions smaller than the irradiating beam, consistent with SEM observations (see Figure S1, and coherence length estimates in Table S1).

The photonic scale nanostructures of the Lycaenid butterfly *Lycaena kasyapa* (Figure S1, p. 1), and the snout weevils (Curculionidae) examined essentially belong to a class of 3D interconnected bicontinuous networks with varying degrees of disorder from triply periodic all the way to amorphous networks. Scales (53 out of 90) of most weevils examined (*e.g.*, *Pachyrrhynchus*, *Chrysolopus*, *Apodrosus* spp.) possessed the single diamond network nanostructure (*Fd-3m*; IUCr cubic space group no. 227; Figures 1g, m, 2a, S1, and Table S1), while scales from 9 taxa (*e.g.*, *Rhinoscapha* sp., *Chloropholus* sp.) exhibited a single gyroid network nanostructure ($I4_132$; IUCr cubic space group no. 214), as documented in butterfly wing scales[7] (Figures 1h, n, 2b, S1, and Table S1). 13 taxa (*e.g.*, *Cubicorhynchus* sp., *Naupactus peregrinus*, *Exopthalmus* spp.) exhibited diffraction patterns with one or more broad, isotropic diffraction rings characteristic of spongy or quasi-ordered interconnected networks (Figure S1, and Table S1). SEM images of *Cubicorhynchus* scales confirmed the presence of a spongy or quasi-ordered network of chitin bars (Figure S1.18). However, *Merimnetes* likely possess an amorphous diamond scale nanostructure as the azimuthal profiles showed a weak 222 peak with a near six-fold symmetry (Figure S1.66). Indeed, the sponge morphology can be thought of as a molten or amorphous form of the bicontinuous cubic morphologies. SAXS of weevil scales also uncovered previously undocumented local variations in nanostructure, sometimes even within a

single scale (see Table S1). These include the presence of both, single gyroid and single diamond symmetries (7 scales; *e.g., Lamprocyphus augustus*, Figure S1.78-81); and both single diamond and face-centered orthorhombic (*Fddd*; IUCr orthorhombic space group no. 70) symmetries (8 scales; *e.g.*, many *Eupholus* sp.) in scales of the same taxa or even within a single scale. In the latter, the presence of the Bragg reflection peaks at $\sqrt{4/3}$ (200) and $\sqrt{20/3}$ (420) could also be interpreted as structural reflections from a sheared or distorted cubic nanostructure with face-centered symmetry (*Fm*-3*m*, IUCr cubic space group no. 225 or the closely related "Zinc-blende" *F*4-3*m*, IUCr cubic space group no. 216)[8]. Indeed, the presence of sharp (111) and (311) reflections and relatively oblong air voids along the (111) plane (*e.g.*, in *Eupholus geoffroyi*) compared to other single diamond scale nanostructures (see Figure S1, p. 38) supports a face-centered orthorhombic (*Fddd* space group) structural assignment, as identified in triblock copolymers[9, 10]. In any case, such nanostructural variations, commonly observed in synthetic soft matter systems, can be caused by shear forces during the desiccation of the apoptosing scale cells, or because of the limited long-range spatial periodic ordering (*i.e.*, finite coherence length) within these soft biological systems[8] (Table S1). Intriguingly, the coexistence of two different lyotropic bicontinuous cubic morphologies (double diamond and double gyroid) within the same membrane bound cellular organelle is already documented in cell biology[11, 12].

By contrast to the "true weevils" (Curculionidae), in scales from the basal weevil taxa[13, 14], *Toxonotus* sp. (Anthribidae) and *Isacantha* sp. (Belidae), we report the presence of quasi-ordered sphere nanostructures from the form-factor fitting of the higher-order peaks in the corresponding azimuthal SAXS profiles (Figure S1, pp. 6, and 10). Similarly, in *Leucochromus imperialis* (Curculionidae: Lixinae), although the scales possess what appears to be an

amorphous network, they are comprised of polydisperse (10%) agglulitinated chitin spheres, which explains the spherical form-factor fringes in the azimuthal profile (Figure S1.115).

In longhorn beetles (Cerambycidae), the photonic scale nanostructures were characterized by the presence of either arrays of discrete chitinous spheres (8 out of 19 scales) or ball-and-strut chitin networks (11 out of 19 scales) with variations in spatial periodic order, connectivity and polydispersity (variation in scatterer size). A single primitive (simple cubic) triply periodic bicontinuous network (*Pm*-3*m*; IUCr cubic space group no. 221) was found in scales of 3 *Sternotomis* species, distinguished by the diagnostic presence of √2 diffraction peak and the characteristic absence of √7 peak (Figures 1i, o, 2c, S1, and Table S1). We identified amorphous simple cubic (*Pm*-3*m*) networks in scales of 2 other *Sternotomis* species (Figure S1.133-134), for which the diffraction peaks were indistinct, despite the periodic order observed in SEM images. Although the nanostructure in green scales of *Sternotomis pulchra* showed simple cubic symmetry (Figure 1i, o, 2c, and S1.130), the red scales from the same specimen possessed a quasi-ordered network, with regions of local simple cubic order (Figure S1.131). A body-centered cubic (bcc) (*Im*-3*m*; IUCr cubic space group no. 229) network of connected chitin spheres was diagnosed in scales of *Prosopocera lactator* (*cf.* 15) (Figures S1.135-136, and Table S1). Notably, the scales from *Sternotomis* and *Prosopocera* exhibit the characteristic (111) plane "wagon-wheel" pattern in SEM images (Figures 1i (inset), and S1.132,134-135). Another class of nanostructure in longhorns comprised of close-packed (amorphous and ordered) arrays of discrete chitin spheres, sometimes with thin necks or rods, *e.g.*, in *Anoplophora* spp., *Phosphorus jansoni* and *Glenea fortunei* (Figures 1j, p, 2d-f, S1, and Table S1). In *Anoplophora*, the quasi-ordered arrays of chitin spheres also exhibited localized regions of *bcc* and *fcc* order within the same scale (Figure S1.120-124), as observed recently in another Lamiine longhorn beetle,

Pseudomyagrus waterhousei[16]. The low polydispersity of the chitin spheres (4.5%) with up to 9 orders of form-factor fringes observed in the azimuthal scattering profiles of *A. versteegi* (Figure S1.122) is remarkable for a biological system[17]. The scale nanostructure in *Rosalia alpina* (Figure S1.117), *Coptomma mirabilis* (Figure S1.118) and *Tmesisternus* sp. (Figure S1.127) was determined to be sponge-like or quasi-ordered networks (as opposed to quasi-ordered spheres), from the lack of correspondence between form factor fits to the higher-order scattering features. Such quasi-ordered networks have recently been identified in the photonic scales of *Sphingnotus mirabilis* (Cerambycidae: Lamiinae: Tmesisternini)[18].

We classified the scale nanostructure in two *Hoplia* species (Scarabaeidae, Figure S1, pp. 3, and 4) as inverse (air pores in chitin) 2D columnar morphology with Bouligand plywood-like (helical) twisted domains[19], and very short coherence lengths (0.6-0.8, Table S1). EM images from refs. 20, 21 exhibited characteristic worm-like or herringbone motifs as well as regions of hexagonally ordered pores, often observed during the transition from lamellar to 2D hexagonal phases in block copolymers[22]. The corresponding azimuthal scattering profiles are characterized by broad diffraction rings, with a shoulder at approximately twice the peak q.

The setae of the cuckoo bee, *Thyreus nitidulus* (Apinae: Melectini) also possessed an inverse 2D twisted columnar nanostructure (Figures 1l, r, 2h, and S1, p. 139), like in scales of *Hoplia* spp[20]. However, an amorphous or quasi-ordered sponge-like morphology (Figures 2g, and S1.138) was identified in setae from a closely related species, *Thyreus pictus*. The ring-like diffraction patterns from setae of both *Thyreus* species indicate isotropic spatial order. However, the second-order scattering peak from setae of *T. nitidulus* is more pronounced than that in *T. pictus* and midway between the expected positions for a hexagonal columnar ($\sqrt{3}$) and a lamellar (2) nanostructure. An inverse 2D hexagonal columnar nanostructure (HEX; *p6mm*, IUCr

hexagonal space group no. 183) consisting of a triangular lattice of air cylinders in solid chitin was confirmed[23] to be present in the setae of the blue-banded bee, *Amegilla cingulata* (Apinae: Anthophorini) (Figures 1k, q, and 2i).

Lastly, we report a perforated multilamellar nanostructure to be responsible for the purple-blue coloration in the setae of 3 tarantula species[24, 25] (Araneae: Theraphosidae; Figure S1.142-145), and an inverse 2D hexagonal columnar nanostructure in the iridescent blue setae of a jumping spider (Figure S1.141), as in the blue-banded bee.

Development of scale nanostructure in longhorn beetles

The rather bulbous nodes or junctions of the simple cubic networks in the scales of *Sternotomis* are more or less spherical in shape (Figures 1i, and S1.130-134), a characteristic of the precursor *P* minimal surface that degenerates into spheres[26], and are of similar sizes to the chitin spheres seen in the scale nanostructures of other long-horned beetle taxa such as *Anoplophora* (Figures 1j, and S1.120-124). However, the former are inter-connected by robust chitin bars, while the latter sometimes have only thin necks connecting adjacent spheres. This structural similarity and the phylogenetic relatedness of long-horned beetles give us a strong clue as to the mechanism by which close-packed or jammed arrays of spheres may develop in photonic scales of *Anoplophora*, *Glenea* and *Phosphorus*. The *P* minimal surface can self-intersect under certain conditions, such as swelling of one of the volumes and under low aqueous volume fractions (*e.g.*, during the desiccation of apoptosing scale cells), causing the enclosed volumes to pinch-off or get disconnected to form degenerate spheres[26-29]. Therefore, a bicontinuous cubic network that is developed under less well-regulated conditions than in

Sternotomis can result in individual chitin spheres, which can self-organize into close-packed arrays according to purely mechanical considerations[30, 31].

SAXS optical reflectance predictions

The SAXS structural data from arthropod photonic scales and setae assayed in this study confirms that the underlying cuticular nanostructures are sufficiently ordered at the appropriate length scales to produce the observed structural colors through constructive interference of scattered light. The single-scattering optical predictions[6, 7] based on SAXS structural data reasonably agree with the measured normal-incidence optical reflectance spectra of the respective nanostructures (Figure S2). However, a full multiple scattering photonic analyses to account for the broader widths of the measured reflection spectra[7] will be presented elsewhere.

Coherence length estimates of arthropod cuticular photonic nanostructures

We calculated the coherence length of the scale and setae photonic nanostructures, from the full widths at half-maximum (FWHM) of the first-order SAXS peaks[6, 7], $\xi \approx 2\pi/\Delta q$ (Supporting Table 1). ξ is a measure of the size of polycrystalline domains in ordered systems[8], or the spatial extent of short-range order in amorphous or quasi-periodic systems[32]. Coherence length estimates from the SAXS data were in good agreement with crystallite domain sizes observed in SEM images (see Figure S1, and Table S1).

MATERIALS AND METHODS

Small angle X-ray scattering (SAXS)

Scales and setae were obtained from museum and purchased arthropod specimens (Table S1) and sandwiched between 0.0025-inch (~63.5 μm) thick adhesive Kapton polyimide tape (McMaster-

Carr catalogue no. 7648A33) for SAXS data collection. Pinhole SAXS (15 μm horizontal x 15 μm vertical) data in transmission geometry were collected at beamline 8-ID-I of the Advanced Photon Source, Argonne National Labs, Chicago, Illinois, USA from individual arthropod scales or setae and indexed as per standard protocol[7]. SAXS data on 7 (out of 140) patches (Table S1) were collected by A.E.S. using a 7 keV beam (1.77 Å, 250 μm horizontal × 100 μm vertical, 7.279 m camera length, exposures of 1-5 s) on a Pilatus1M detector at the SAXS/WAXS beamline of the Australian Synchrotron, Victoria, Australia, while SAXS data on a further 3 scales (Table S1) were collected using a 7.35 keV beam (1.68 Å, 50 μm horizontal × 50 μm vertical, 9.24 m camera length, 50 x 0.1 s exposures) on a Pilatus2M detector at beamline I22 of the Diamond Light Source, Didcot, UK.

Microscopy and Imaging

Light micrographs of the scale or setae-covered integument from arthropod specimens were obtained at various magnifications on a Nikon stereo light microscope using a 40x objective and recorded using a Moticam 2300, 3.0 Megapixel digital color camera. For scanning electron microscopy (SEM), fractured samples were gold-coated and studied on a Hitachi SU-70, Hitachi-S4300 and a Philips XL 30 environmental SEM, at a range of tilt angles from -10° to 45°. We followed standard embedding procedures for transmission electron microscopy (TEM)[33].

Parameterisation of SAXS data

The SAXS diffraction patterns from arthropod scale and setae nanostructures exhibit either concentric spots or ring-like features (Figures 1m-r, and S1). Exploiting the circular symmetry of the SAXS diffraction patterns, we azimuthally integrated them using the XPCSGUI package

(supplied by APS beamline 8-ID) after masking out the beam stop pixels and artifacts, to obtain profiles of the scattered intensity as a function of scattering wavevector, *I(q)*, at 200 equal *q*-partitions or spatial frequency bins (Figures 2, and S1)[6]. The azimuthally averaged profiles were deconvolved, or peak-fitted, to estimate the peak *q* value, intensity, and the full width at half maximum (FWHM) of the scattering peaks, using the peak-fitting software, Fityk (version 0.9.8)[34] on a Macintosh platform. We used a Porod background (q^{-4} dependence) and the split pseudo-Voigt function with a Levenberg-Marquardt least square method to fit the scattering features present in the azimuthal profiles. The pseudo-Voigt function is a combination of Gaussian and Lorentzian (Cauchy) type peak profiles that is used to closely approximate X-ray scattering peaks[3, 35]. The split pseudo-Voigt accommodates any asymmetry in peak shapes.

Spectrophotometry and single-scattering reflectance predictions

Normal incidence reflectance spectra from a 3 mm^2 patch of the arthropod integument were collected as in ref. 33.

The structurally predicted single-scattering optical reflectance follows from Bragg's law[6, 7] and is given by mapping the X-ray scattering intensity from scattering wavevector to wavelength space:

$$\lambda = 2\, n_{avg} \left(\frac{2\pi}{q} \right) \sin\theta \qquad (1)$$

where θ, the angle of incidence is 90° for back-reflection or normal incidence, n_{avg} is the average or effective refractive index of the nanostructure and q is the scattering wavevector obtained from the azimuthally averaged SAXS scattering profile.

Figure S1. Morphology of arthropod cuticular photonic nanostructures assayed in this study (figures provided in a separate file nl5b00201_si_002.pdf).

Bottom left: SAXS patterns (unmasked; original images 1340 x 1300 pixels). The false color scale corresponds to the logarithm of scattering intensity. The concentric white circles denote the expected locations of the scattering peaks for the indexed space group; Bottom center: Structural diagnoses of normalized, azimuthally-averaged SAXS profiles integrated from 2D SAXS patterns. Vertical lines denote expected Bragg peak positional ratios for various crystallographic space groups. Numbers above the vertical lines are squares of the moduli of the Miller indices (*hkl*) for the allowed reflections of the cubic space-groups. The normalized positional ratios of the scattering peaks are indexed to the predictions of specific crystallographic space groups or symmetries following IUCr conventions[36]; Bottom right: Indexing of the azimuthally averaged profiles of the respective 2D SAXS patterns of photonic nanostructures, using the plot of the moduli of the *hkl* Miller indices of the Bragg peaks against the corresponding reciprocal lattice spacing, *S*. The observed peaks (solid black circles) are shown alongside the theoretically allowed reflections for the assigned crystallographic space group symmetries. Linearity and zero intercepts of the plot confirm the cubic aspect of the nanostructures, while the slope gives an estimate of the lattice parameter, *a*.

Where available or pertinent, we also provide the following additional information:

Top left: SEM images with scale bars; Top center: Light micrograph images; Top right: Habitus images of the arthropod taxa, and spherical form-factor fits to diffraction fringes.

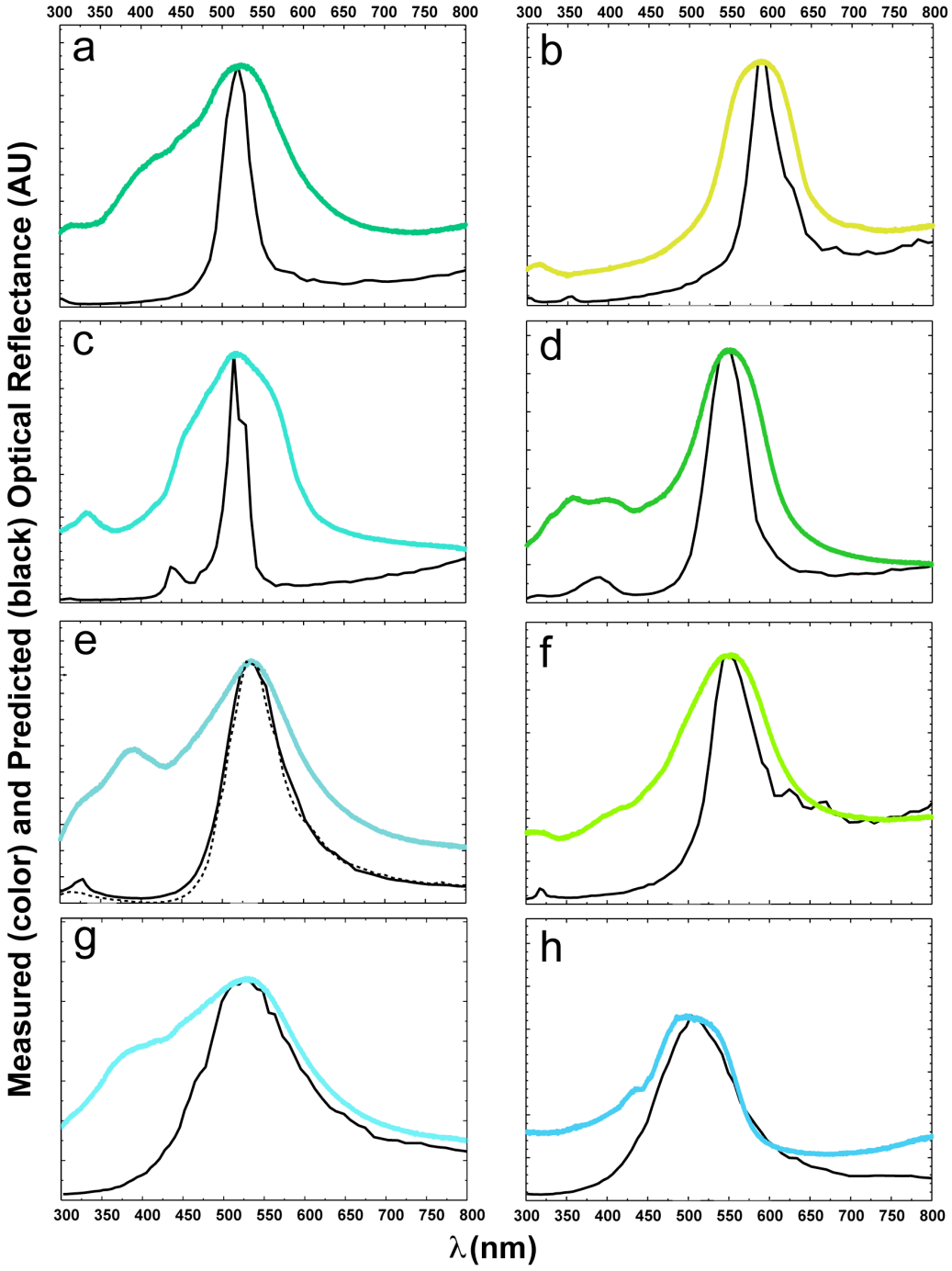

Figure S2. Representative normal-incidence optical reflectance spectra with single-scattering SAXS nanostructural predictions for arthropod photonic nanostructures.

(**a**) *Rhinoscapha* sp. (Curculionidae), $I4_132$; (**b**) *Lamprocyphus augustus* (Curculionidae), *Fd*-3*m* + $I4_132$; (**c**) *Eupholus quintaenia* (Curculionidae), *Fd*-3*m*; (**d**) *Sternotomis pulchra* (green scales)

(Cerambycidae), *Pm*-3*m*; (**e**) *Anoplophora graafi* (Cerambycidae), quasi-ordered + *fcc* opal; (**f**) *Amegilla cingulata* (Apidae), inverse 2D hexagonal columnar; (**g**) *Thyreus pictus* (Apidae), sponge; and (**h**) *Thyreus nitidulus* (Apidae), inverse 2D twisted columnar. In (**e**), the solid black curve is the reflectance predicted from an ordered region of close-packed chitin spheres, whereas the dotted curve is from a quasi-ordered region. Note that the agreement of the single-scattering predictions to the optical measurements increases with decreasing coherence length of the nanostructure (*i.e.*, as the structural peak width increases or optical saturation decreases), in going from ordered to quasi-ordered systems.

SUPPORTING REFERENCES

1. Shearman, G. C.; Ces, O.; Templer, R. H.; Seddon, J. M. *J. Phys.: Condens. Matter* **2006,** 18, S1105-S1124.

2. Glatter, O.; Kratky, O., *Small Angle X-ray Scattering*. Second ed.; Academic Press: London, 1983.

3. Svergun, D. I.; Feigin, L. A.; Taylor, G. W., *Structure analysis by small-angle x-ray and neutron scattering*. Plenum Press: New York, 1987; p xiii, 335 p.

4. Hallam, B. T.; Hiorns, A. G.; Vukusic, P. *Appl. Optics* **2009,** 48, 3243-3249.

5. Vukusic, P.; Hallam, B.; Noyes, J. *Science* **2007,** 315, 348.

6. Saranathan, V.; Forster, J. D.; Noh, H.; Liew, S. F.; Mochrie, S. G. J.; Cao, H.; Dufresne, E. R.; Prum, R. O. *J. R. Soc., Interface* **2012,** 9, 2563-2580.

7. Saranathan, V.; Osuji, C. O.; Mochrie, S. G. J.; Noh, H.; Narayanan, S.; Sandy, A.; Dufresne, E. R.; Prum, R. O. *P. Natl. Acad. Sci. USA* **2010,** 107, 11676-11681.

8. Förster, S.; Timmann, A.; Schellbach, C.; Frömsdorf, A.; Kornowski, A.; Weller, H.; Roth, S. V.; Lindner, P. *Nat. Mater.* **2007,** 6, 888-893.

9. Tyler, C. A.; Morse, D. C. *Phys Rev Lett* **2005,** 94, 208302.

10. Bailey, T. S.; Hardy, C. M.; Epps, T. H., III; Bates, F. S. *Macromolecules* **2002,** 35 7007-7017.

11. Deng, Y.; Marko, M.; Buttle, K. F.; Leith, A.; Mieczkowski, M.; Mannella, C. A. *J. Struct. Biol.* **1999,** 127, 231-239.

12. Almsherqi, Z. A.; Landh, T.; Kohlwein, S. D.; Deng, Y. R. *Int. Rev. Cell Mol. Biol.* **2009,** 274, 275-342.

13. McKenna, D.; Sequeira, A.; Marvaldi, A.; Farrell, B. *P. Natl. Acad. Sci. USA* **2009,** 106, 7083-7088.

14. Hunt, T.; Bergsten, J.; Levkanicova, Z.; Papadopoulou, A.; John, O. S.; Wild, R.; Hammond, P. M.; Ahrens, D.; Balke, M.; Caterino, M. S.; Gomez-Zurita, J.; Ribera, I.; Barraclough, T. G.; Bocakova, M.; Bocak, L.; Vogler, A. P. *Science* **2007,** 318, 1913-6.

15. Colomer, J.-F.; Simonis, P.; Bay, A.; Cloetens, P.; Suhonen, H.; Rassart, M.; Vandenbem, C.; Vigneron, J. P. *Phys. Rev. E: Stat., Nonlinear, Soft Matter Phys.* **2012,** 85, 011907.

16. Simonis, P.; Vigneron, J. P. *Phys. Rev. E: Stat., Nonlinear, Soft Matter Phys.* **2011,** 83, 011908.

17. Dingenouts, N.; Ballauff, M. *Macromolecules* **1998,** 31, 7423-7429.

18. Dong, B. Q.; Zhan, T. R.; Liu, X. H.; Jiang, L. P.; Liu, F.; Hu, X. H.; Zi, J. *Phys. Rev. E: Stat., Nonlinear, Soft Matter Phys.* **2011,** 84, 011915.

19. Bouligand, Y. *Tiss. Cell* **1972,** 4, 189-217.

20. Vigneron, J. P.; Colomer, J. F.; Vigneron, N.; Lousse, V. *Phys. Rev. E: Stat., Nonlinear, Soft Matter Phys.* **2005,** 72, 061904.

21. Rassart, M.; Simonis, P.; Bay, A.; Deparis, O.; Vigneron, J. P. *Phys. Rev. E: Stat., Nonlinear, Soft Matter Phys.* **2009,** 80, 031910.

22. Knoll, A.; Lyakhova, K. S.; Horvat, A.; Krausch, G.; Sevink, G. J.; Zvelindovsky, A. V.; Magerle, R. *Nat. Mater.* **2004,** 3, 886-91.

23. Fung, K. K. *Microsc. Microanal.* **2005,** 11, 1202-1203.

24. Foelix, R.; Erb, B.; Hill, D., Structural Colors in Spiders. In *Spider Ecophysiology*, Nentwig, W., Ed. Springer Berlin Heidelberg: 2013; pp 333-347.

25. Simonis, P.; Bay, A.; Welch, V. L.; Colomer, J. F.; Vigneron, J. P. *Opt. Express* **2013,** 21, 6979-6996.

26. Grosse-Brauckmann, K. *J. R. Soc., Interface focus* **2012,** 2, 582-588.

27. Lambert, C. A.; Radzilowski, L. H.; Thomas, E. L. *Philos. Trans. R. Soc. A* **1996,** 354, 2009-2023.

28. Shearman, G. C.; Khoo, B. J.; Motherwell, M. L.; Brakke, K. A.; Ces, O.; Conn, C. E.; Seddon, J. M.; Templer, R. H. *Langmuir* **2007,** 23, 7276-7285.

29. Moon, J. H.; Xu, Y. G.; Dan, Y. P.; Yang, S. M.; Johnson, A. T.; Yang, S. *Adv. Mater.* **2007,** 19, 1510-1514.

30. Lois, G.; Blawzdziewicz, J.; O'Hern, C. S. *Phys. Rev. Lett.* **2008,** 100, 028001.

31. Kansal, A. R.; Torquato, S.; Stillinger, F. H. *Phys. Rev. E: Stat., Nonlinear, Soft Matter Phys.* **2002,** 66, 041109.

32. Noh, H.; Liew, S. F.; Saranathan, V.; Mochrie, S. G. J.; Prum, R. O.; Dufresne, E. R.; Cao, H. *Adv. Mater.* **2010,** 22, 2871-2880.

33. Prum, R. O.; Quinn, T.; Torres, R. H. *J. Exp. Biol.* **2006,** 209, 749-765.

34. Wojdyr, M. *J. Appl. Crystallogr* **2010,** 43, 1126-1128.

35. Glatter, O.; Kratky, O., *Small Angle X-ray Scattering*. Academic Press: London ; New York, 1982; p 515 p.

36. Hahn, T., The 230 space groups. In *IUCr International Tables for Crystallography* , Springer: 2006; Vol. A, Ch. 7.1, pp 112-717.

37. Onslow, H. *Phil. Trans. R. Soc., B* **1923,** 211, 1-74.

38. Mason, C. W. *J. Phys. Chem.* **1926,** 31, 321-354.

39. Wilts, B. D.; Michielsen, K.; De Raedt, H.; Stavenga, D. G. *J. R. Soc., Interface* **2011,** 9, 1609-14.

40. Deparis, O.; Vigneron, J. P. *Mater. Sci. Eng. B: Adv.* **2010,** 169, 12-15.

41. Wilts, B. D.; Michielsen, K.; Kuipers, J.; De Raedt, H.; Stavenga, D. G. *Proc. R. Soc. B* **2012,** 279, 2524-2530.

42. Wilts, B. D.; IJbema, N.; Michielsen, K.; De Raedt, H.; Stavenga, D. G. *MRS Online Proc. Libr.* **2013,** 1504.

43. Jorgensen, M. R.; Bartl, M. H. *J. Mater. Chem.* **2011,** 21, 10583-10591.

44. Pouya, C.; Stavenga, D. G.; Vukusic, P. *Opt. Express* **2011,** 19, 11355-11364.

45. Galusha, J. W.; Richey, L. R.; Jorgensen, M. R.; Gardner, J. S.; Bartl, M. H. *J. Mater. Chem.* **2010,** 20, 1277-1284.

46. Galusha, J. W.; Richey, L. R.; Gardner, J. S.; Cha, J. N.; Bartl, M. H. *Phys. Rev. E: Stat., Nonlinear, Soft Matter Phys.* **2008,** 77, 2-5.

47. Welch, V.; Lousse, V.; Deparis, O.; Parker, A.; Vigneron, J. P. *Phys. Rev. E: Stat., Nonlinear, Soft Matter Phys.* **2007,** 75, 1-9.

48. Parker, A. R.; Welch, V. L.; Driver, D.; Martini, N. *Nature* **2003,** 426, 786-787.

49. Seago, A. E.; Brady, P.; Vigneron, J.-P.; Schultz, T. D. *J. R. Soc., Interface* **2009,** 6, S165-84.

50. Gorb, S., Insect-Inspired Technologies: Insects as a Source for Biomimetics. In *Insect Biotechnology*, Vilcinskas, A., Ed. Springer Netherlands: 2011; Vol. 2, pp 241-264.

51. Tamanis, E.; Mihailova, I.; Valainis, U.; Gerbreders, V. *Acta. Biol. Univ. Daugavp.* 12, 58-64.

52. Ghiradella, H. *Ann. Entomol. Soc. Am.* **1984,** 77, 637-645.

53. McNamara, M. E.; Saranathan, V.; Locatelli, E. R.; Noh, H.; Briggs, D. E.; Orr, P. J.; Cao, H. *J. R. Soc., Interface* **2014,** 11, 20140736.

54. Dong, B. Q.; Liu, X. H.; Zhan, T. R.; Jiang, L. P.; Yin, H. W.; Liu, F.; Zi, J. *Opt. Express* **2010,** 18, 14430-14438.

55. Liu, F.; Dong, B. Q.; Liu, X. H.; Zheng, Y. M.; Zi, J. *Opt. Express* **2009,** 17, 16183-16191.

56. Van Hooijdonk, E.; Barthou, C.; Vigneron, J. P.; Berthier, S. *J. Lumin.* **2013,** 136, 313-321.

57. Ingram, A. L.; Deparis, O.; Boulenguez, J.; Kennaway, G.; Berthier, S.; Parker, A. R. *Arthropod. Struct. Dev.* **2011,** 40, 21-25.

58. Ingram, A. L.; Ball, A. D.; Parker, A. R.; Deparis, O.; Boulenguez, J.; Berthier, S. *J. Arachnol.* **2009,** 37, 68-71.

59. Land, M. F.; Horwood, J.; Lim, M. L. m.; Li, D. *Proc. R. Soc. B* **2007,** 274, 1583-1589.

60. Townsend, V. R.; Felgenhauer, B. E. *J. Morphol.* **1999,** 240, 77-92.

61. Forster, J. D.; Noh, H.; Liew, S. F.; Saranathan, V.; Schreck, C. F.; Yang, L.; Park, J. G.; Prum, R. O.; Mochrie, S. G. J.; O'Hern, C. S.; Cao, H.; Dufresne, E. R. *Adv. Mater.* **2010,** 22, 2939-2944.

Supporting Table S1

A summary of the SAXS structural and optical reflectance properties of the photonic nanostructures assayed from distinctly colored scales and setae (N = 140) of a lycaenid butterfly, a bee-fly, various weevils, longhorn beetles, bees, tarantulas and jumping spiders.

Taxon	Accession nos	Locality	Date Collected	Anatomy	q_{pk} ± stdev (nm^{-1}) (N, no. of assays)	Lattice parameter[a] a (nm)	Peak width, Δq ± stdev (nm^{-1})	Cohe-rence length[b] ξ (μm)	Nanostructure[c] [references]	Reflectance peak (FWHM) (nm)	n_{avg} (ϕ)[d]
Class Insecta											
Order Lepidoptera											
Family Lycaenidae (blues and coppers)											
Subfamily Lycaeninae											
[f]*Lycaena kasyapa* (Moore 1865)	OUNHM #885	Kashmir	Jul-Sep1962	pale bluish-green ventral wing scale	0.02546 (1)	349.05	0.00355	1.8	*SG		
Order Coleoptera											
Family Scarabaeidae (scarabs)											
Subfamily Melolonthinae											
Polyphylla decemlineata (Say 1823)	YPM 707793	Cave Cr. Ranch, Arizona	7-Aug-1957	white elytron scale					not structured		
Cyphochilus sp.	YPM 706546	China	26-May-1908	white elytron scale					not structured[4, 5]		
Tribe Hopliini											
Hoplia coerulea (Drury	OUNHM	Dourdou, France	8-Jul-1989	blue elytron	0.03594±0.00009 (2)	174.83	0.00807±0.00102	0.8	inverse 2D		

1773)				scale						twisted columnar[20]		
Hoplia sp.	OUNHM	Prior, Germany	6-Jun-1909	pale green elytron scale	0.03189±0.00022 (3)	196.80	0.01066±0.00026	0.6	inverse 2D twisted columnar[20]			
Family Anthribidae												
Subfamily Anthribiinae												
Tribe Anthribini												
Trigonothinus sp.	CSIRO ANIC			dull greenish elytron scale					not structured			
Tribe Platystomini												
Toxonotus sp.	CSIRO ANIC			pale reddish-brown elytron scale	0.02012±0.00104 (1)	313.03	0.00595±0.00088	1.1	*quasi-ordered spheres	861.7 (632.0)	1.38 (0.68)	
Subfamily Urodontinae												
Urodontus sp.	CSIRO ANIC			greenish-brown elytron scale					not structured			
Bruchela sp.	CSIRO ANIC			greenish-white elytron scale					not structured			
Family Attelabidae												
Subfamily Rhynchitinae												
Tribe Rhynchitini												
Rhynchites sp.	CSIRO ANIC			reddish-green elytron scale					not structured			
Family Belidae												
Subfamily Belinae												

Tribe Belini									
Isacantha sp.	CSIRO ANIC	reddish-green elytron scale	0.02137±0.00097 (5)	294.52	0.00862±0.00068	0.7	*quasi-ordered spheres	840.7 (612.5)	1.43 (0.77)
Family Caridae									
Car sp.	CSIRO ANIC	dull greenish elytron scale					not structured		
Family Erirhinidae									
Echinocnemus sp.	CSIRO ANIC	pale greenish-white elytron scale					not structured		
Aonychus bicruciatus (Lea 1905)	CSIRO ANIC	greenish-white leg scale					not structured		
Family Nemonychidae									
Subfamily Nemonychinae									
Nemonyx sp.	CSIRO ANIC	greenish-white elytron scale					not structured		
Family Curculionidae (weevils)									
Incertae sedis									
Misophrice sp.	CSIRO ANIC	yellowish-green elyron scale	0.02421±0.00040 (2)	454.87	0.00373±0.00222	1.7	SD		
Subfamily Brachycerinae									
Tribe Brachycerini									

Brachycerus sp.	CSIRO ANIC			greenish-brown elytron scale					not structured		
Tribe Bagoini											
Bagous sp.	CSIRO ANIC			greenish-brown elytron scale					not structured		
Subfamily Cyclominae											
Tribe Amycterini											
Cubicorhynchus maculatus (Macleay 1865)	CSIRO ANIC	Mallee District, Victoria, Australia	No data	rose-brown elytron scale	0.01746 (1)	359.92	0.00668	0.9	amorphous network	804.0 (195.8)	1.12 (0.21)
Tribe Aterpini											
Aesiotes sp.	CSIRO ANIC	Sydney, NSW, Australia	1922	brown elytron scale	0.01795±0.00014 (6)	606.43	0.00196±0.00016	3.2	SD	814.2 (343.9)	1.16 (0.29)
Chrysolopus sp.	CSIRO ANIC	Canberra, Australia	1979	green elytron scale	0.02541±0.00055 (5)	428.51	0.00233±0.00109	2.7	SD	551.9 (150.5)	1.12 (0.20)
Chrysolopus sp.	CSIRO ANIC	Currarong, NSW, Australia	Jan 1967	blue elytron scale	0.02693±0.00041 (5)	404.20	0.00375±0.00150	1.7	SD		
Chrysolopus sp.	YPM 707800	Wasile Dt., Indonesia	10-Oct-1970	green elytron scale	0.02438±0.00030 (5)	446.48	0.00280±0.00037	2.2	SD	538.8 (176.5)	1.05 (0.08)
Tribe Diabathrariini											
Aphanonyx setulosus (Marshall 1935)	CSIRO ANIC			dull greenish leg scale					not structured		
Tribe Listroderinii											
Steriphus sp.	CSIRO ANIC			pale reddish-green elytron scale					not structured		
Tribe Viticiini											
gen. et sp. nov.	CSIRO ANIC			yellowish-	0.02211±0.00082 (3)	492.76	0.00212±0.00073	3.0	SD		

				green elytron scale							
Subfamily Entiminae											
gen. et sp. nov.	YPM 707820	Ledesma, Argentina	4-Apr-1922	yellow-green elytron scale	0.02333±0.00035 (4)	380.96	0.00241±0.00080	2.6	SG	581.5 (149.6)	1.08 (0.14)
Tribe Celeuthetini											
gen. et sp. nov.	YPM 707823	Solomon Islands	9-Aug-1959	yellowish-green elytron scale	0.02488±0.00080 (3)	437.77	0.00217±0.00101	2.9	SD	586.2 (94.0)	1.16 (0.28)
Pyrgops aurocinctus (Lacordaire 1863)	OUNHM	Philippines	No data	bluish-green elytron scale	0.02392±0.00026 (3)	454.98	0.00262±0.00123	2.4	SD		
Tribe Cratopini											
Cratopus ditissimus (Schoenherr 1840)	OUNHM	No data	presented 1911	green elytron scale	0.02280±0.00036 (4)	477.34	0.00243±0.00030	2.6	SD		
Tribe Cyphicerini											
Myllocerus tatei (Blackbourn 1896)	CSIRO ANIC	Western Australia	May 1968	yellow-green elytron scale	0.02476±0.00013 (4)	439.57	0.00182±0.00029	3.4	SD	587.8 (143.0)	1.16 (0.28)
Subtribe Cyphicerina											
Peltotrachelus pubescens (Marshall 1917)	OUNHM	“British India”	31-Mar-1909	pale green elytron scale	0.02228±0.00114 (3)	282.47	0.00809±0.00334	0.8	*amorphous network		
Tribe Entimini											
Polyteles coelestinus (Perty 1832)	OUNHM	Brasil	No data	turquoise elytron scale	0.02472±0.00044 (7)	440.28	0.00240±0.00051	2.6	SD		
Rhigus nigroparsus (Perty 1832)	OUNHM	Brasil	No data	turquoise elytron scale	0.01632±0.00012 (4)	544.42	0.00145±0.00058	4.3	SG		
Entimus imperialis (Forster 1771)	OUNHM	Brasil	No data	opalescent scale	0.02334±0.00114 (3)	466.98	0.00317±0.00183	5.9	SD[37-42]		
Tribe Episomini											
Catamonus rufipes	OUNHM	Brasil	presented	blue-green	0.02428±0.00059 (3)	448.37	0.00273±0.00055	2.3	SD		

(Boheman 1845)			1911	elytron scale							
Tribe Eudiagogini											
Eudiagogus episcopalis (Schoenherr 1840)	OUNHM	Porto Alegre, Brasil	No data	red elytron scale	0.02214±0.00001 (2)	491.55	0.00254±0.00057	2.5	SD[43]		
Eudiagogus episcopalis (Schoenherr 1840)	OUNHM	Porto Alegre, Brasil	No data	orange elytron scale	0.02074 (1)	524.70	0.00368	1.7	SD[43]		
Tribe Eupholini											
Eupholus geoffroyi (Guérin-Méneville 1830)	YPM 707795	W. Sepik, Papua New Guinea	Nov 1986	bluish-green elytron scale	0.02525±0.00043 (10)	431.12	0.00155±0.00051	4.1	*SD(4) + *Fddd*(6) [37, 38, 42, 44, 45]	518.3 (127.8)	1.04 (0.07)
Eupholus bennetti (Gestro 1876)	YPM 707794	Morobe, Papua New Guinea	No data	blue elytron scale	0.03107±0.00067 (8)	350.47	0.00295±0.00049	2.1	SD[37, 38, 42, 44, 45]	411.8 (176.4)	1.02 (0.03)
Eupholus bennetti (Gestro 1876)	YPM 707794	Morobe, Papua New Guinea	No data	pearly bluish elytron scale	0.03682 (1)	170.66	0.03386	0.2	amorphous network		
Eupholus quintaenia (Heller 1915)	YPM 707797	W. Sepik, Papua New Guinea	Jun 1988	emerald green elytron scale	0.02496±0.00060 (12)	435.75	0.00202±0.00083	3.1	*SD(11) + *Fddd*(1)[37, 38, 42, 44, 45]	516.4 (127.7)	1.03 (0.04)
Eupholus schoenherri (Boisduval 1835)	YPM 707798	W. Sepik, Papua New Guinea	Jun 1988	bluish-green elytron scale	0.02537±0.00047 (12)	429.10	0.00236±0.00141	2.7	*SD(7) + *Fddd*(5) [37, 38, 42, 44, 45]	560.1 (133.6)	1.13 (0.23)
Eupholus schoenherri (Guérin-Méneville 1830)	YPM 708909	Kamu valley, Indonesia	16 Aug - 13 Sep 1962	bluish-green elytron scale	0.02544±0.00074 (4)	424.28	0.00228±0.00073	2.8	SD[37, 38, 42, 44, 45]	506.9 (113.57)	1.03 (0.05)
Eupholus schoenherri (Guérin-Méneville 1830)	YPM 708909	Kamu valley, Indonesia	16 Aug - 13 Sep 1962	yellowish-green elytron scale	0.02406 (1)	452.36	0.00233	2.7	SD[37, 38, 42, 44, 45]	576.1 (151.9)	1.10 (0.18)
Eupholus sp.	YPM 708914	Kamu valley, Indonesia	Aug - Sep 1962	orange elytron scale	0.02251±0.00031 (8)	483.59	0.00189±0.00085	3.3	SD[37, 38, 42, 44, 45]	615.0 (193.5)	1.10 (0.18)
Eupholus sp.	YPM 708914	Kamu valley, Indonesia	Aug - Sep 1962	pinkish-red elytron scale	0.02111±0.00025 (2)	515.55	0.00154±0.00037	4.1	SD[37, 38, 42, 44, 45]		
[e]*Eupholus* sp.	CSIRO ANIC	Papua New Guinea	1960	blue elytron scale	0.02771 (1)	392.72	0.00406	1.5	SD[37, 38, 42, 44, 45]		
Eupholus (*latreillei*) *schoenherrii petiti*	OUNHM	Ceram or New Guinea	No data	bluish-green elytron scale	0.03006 (1)	362.06	0.00182	3.5	*SD[37, 38, 42, 44, 45]		

(Guérin-Méneville 1841)											
Eupholus (*latreillei*) *schoenherrii petiti* (Guérin-Méneville 1841)	OUNHM	Ceram or New Guinea	No data	yellowish-green elytron scale	0.02400±0.00081 (3)	453.85	0.00174±0.00035	3.6	SD[37, 38, 42, 44, 45]		
Eupholus brownii (Bates 1877)	OUNHM	New Britain	No data	dull yellow elytron scale	0.02986±0.00113 (2)	210.61	0.00383±0.00166	1.6	*amorphous network[37, 38, 42, 44, 45]		
Danae (*Rhinoscapha*) sp.	OUNHM	No data	No data	light blue elytron scale	0.02534±0.00032 (3)	429.59	0.00269±0.00068	2.3	SD		
Rhinoscapha sp.	purchased	New Br., Papua New Guinea	23-Oct-1992	bluish-green elytron scale	0.02557±0.00037 (13)	347.27	0.00312±0.00118	2.0	SG	519.5 (121.5)	1.06 (0.10)
Celebia iligana (Schulze 1922)	CSIRO ANIC	Dinagat Islands, Phillippines	Nov 1992	green elytron scale	0.02314±0.00079 (4)	459.75	0.00189±0.00040	3.3	SD	566.8 (103.5)	1.04 (0.08)
Gymnopholus sp.	CSIRO ANIC	Papua New Guinea	Apr 1974	green elytron scale	0.02534±0.00057 (7)	420.70	0.00235±0.00066	2.7	*SD(6) + *Fddd*(1)	556.3 (99.7)	1.12 (0.21)
Tribe Eustylini											
*Eustales adamantinus (*Schoenherr 1826*)*	OUNHM	Brasil	presented 1911	green elytron scale	0.02438±0.00025 (2)	446.35	0.00171±0.00105	3.7	*SD(1) + *Fddd*(1)		
*Eustales circumdictus (*Schoenherr 1826*)*	OUNHM	Brasil	presented 1911	orange-green elytron scale	0.02358±0.00030 (3)	461.51	0.00255±0.00085	2.5	SD		
Exopthalmus bivittatus (Schoenherr 1834)	OUNHM	St. Thomas	presented 1911	white elytron scale	0.01635±0.00015 (4)	384.38	0.00327±0.00092	1.9	*amorphous network		
Exopthalmus crassicornis (Kirsch 1867)	OUNHM	Neotropics	presented 1911	pale green elytron scale	0.02814 (1)	223.31	0.00442	1.4	*amorphous network		
Diaprepes abbreviatus (Linnaeus 1758)	OUNHM	Guadeloupe	presented 1911	light green elytron scale	0.02416 (1)	450.48	0.00325	1.9	SD		
Prepodes vittatus (Schoenherr 1834)	OUNHM	Jamaica	presented 1911	silvery orange-green elytron scale	0.02212 (1)	491.94	0.00259	2.4	SD		
Prepodes regalis	OUNHM	St. Domingo	presented	pinkish-red	0.02195±0.00032 (6)	495.94	0.00193±0.00141	3.3	*SD(2) +		

(Schoenherr 1834)			1911	elytron scale					*Fddd*(4)		
Prepodes regalis (Schoenherr 1834)	OUNHM	St. Domingo	presented 1911	green elytron scale	0.02643 (1)	336.14	0.00148	4.3	SG		
Tribe Geonemini											
Lachnopus aurifer (Drury 1773)	OUNHM	Jamaica	presented 1911	greenish-yellow elytron scale	0.02206±0.00011 (2)	402.72	0.00194±0.00022	3.2	SG		
Tribe Laparocerini											
Merimnetes sp.	CSIRO ANIC	Tasmania, Australia	Feb 1980	reddish-orange elytron scale	0.02065 (1)	304.27	0.00811	0.8	*amorphous network	774.4 (282.4)	1.27 (0.49)
Tribe Lordopini											
Diaprosomus magnificus (Heyne et Taschenberg 1908)	OUNHM	Brasil	No data	blue-green elytron scale	0.02346±0.00040 (2)	378.80	0.00166±0.00035	3.8	SG		
Tribe Naupactini											
Naupactus sp.	CSIRO ANIC	Chelgiup Ck, W. Australia	May 2000	dull green elytron scale	0.02029±0.00031 (6)	537.69	0.00401±0.00082	1.6	SD		
Naupactus peregrinus (Buchanan 1939)	CSIRO ANIC	Jerry's Plains, NSW, Australia	Jan 1986	greenish-brown elytron scale	0.01862±0.00016 (3)	579.09	0.00573±0.00160	1.1	*amorphous SD network	724.3 (337.9)	1.07 (0.13)
Platyomus cultricollis (Schoenherr 1840)	OUNHM	Brasil	presented 1911	dull brownish-red elytron scale	0.01878±0.00018 (3)	579.55	0.00217±0.00015	2.9	SD[37]		
Platyomus mutabilis (Schoenherr 1840)	OUNHM		presented 1911	pale green elytron scale	0.01701±0.00016 (4)	639.87	0.00215±0.00049	2.9	SD[37]		
Lamprocyphus (*Cyphus*) *germari* (Boheman 1833)	OUNHM	Brasil	presented 1911	green elytron scale	0.02444±0.00028 (4)	434.90	0.00277±0.00148	2.3	*SD(3) + SG[46]		
Lamprocyphus (*Cyphus*) *spixi* (Perty 1833)	OUNHM	Brasil	presented 1911	blue elytron scale	0.02500±0.00048 (5)	411.15	0.00412±0.00051	1.5	*SD(2) + SG[46]		
Lamprocyphus (*Cyphus*)	OUNHM	Brasil	presented 1911	dull pink elytron scale	0.01735 (1)	569.74	0.00381	1.6	*SD + SG[46]		

margaritaceus (Sturm 1826)											
Lamprocyphus (*Cyphus*) *augustus* (Illiger 1802)	OUNHM	Brasil	presented 1911	green elytron scale	0.02415±0.00043 (3)	395.06	0.00199±0.00069	3.2	*SD(1) + SG(2)[46]		
Lamprocyphus augustus (Illiger 1802)	purchased	Brazil	No data	golden green elytron scale	0.02556±0.00049 (17)	374.96	0.00220±0.00047	2.9	*SD(3) + SG(8)[46]	587.1 (111.8)	1.19 (0.34)
gen. et sp. nov.	YPM 707824	Sao Paulo, Brazil	Jan 1904	blue-green elytron scale	0.02383±0.00018 (3)	456.72	0.00260±0.00071	2.4	SD	565.4 (152.6)	1.07 (0.15)
Tribe Pachrrhynchini											
Pachyrrhynchus yamianus (Kano 1929)	purchased	No data	No data	green elytron scale	0.02534±0.00037 (8)	429.53	0.00195±0.00031	3.2	SD[45, 47-49]	581.8 (109.1)	1.17 (0.31)
Pachyrrhynchus reticulatus (Waterhouse 1841)	YPM 707802	Aurora, Philippines	26-Apr-1953	green elytron scale	0.02511±0.00042 (8)	433.43	0.00249±0.00086	2.5	SD[45, 47-49]	576.5 (103.7)	1.15 (0.27)
Pachyrrhynchus reticulatus (Waterhouse 1841)	YPM 707796	Luzon, Philippines	26-Apr-1953	reddish-orange elytron scale	0.02252±0.00035 (6)	468.39	0.00203±0.00047	3.1	*SD(4) + SG[45, 47-49]	652.5 (127.9)	1.17 (0.30)
Pachyrrhynchus pulchellus (Schultze 1922)	YPM 707796	Luzon, Philippines	8-May-1976	pale green elytron scale	0.02689±0.00050 (9)	405.19	0.00433±0.00073	1.5	SD[45, 47-49]	523.0 (182.8)	1.12 (0.21)
[e]*Pachyrrhynchus orbifer* (Waterhouse 1841)	CSIRO ANIC	Manila, Philippines	1905	green elytron scale	0.02424 (1)	449.00	0.00385	1.6	SD[45, 47-49]		
Pachyrrhynchus orbifer (Waterhouse 1841)	OUNHM	Manila, Philippines	1905	orange-green elytron scale	0.02318±0.00018 (4)	469.50	0.00319±0.00128	2.0	SD[45, 47-49]		
Pachyrrhynchus gemmatus (Waterhouse 1841)	OUNHM	Philippines	1841-1875	pinkish-red elytron scale	0.02367±0.00053 (2)	459.89	0.00084±0.00045	7.5	SD[45, 47-49]		
Pachyrrhynchus gemmatus (Waterhouse 1841)	OUNHM	Philippines	1841-1875	green elytron scale	0.02591±0.00067 (3)	422.74	0.00345±0.00174	1.8	*SD(1) + *Fddd*(1) [45, 47-49]		
Pachyrrhynchus venustus (Waterhouse 1841)	OUNHM	Manila, Philippines	1841-1875	dull green elytron scale	0.02284±0.00010 (2)	476.59	0.00266±0.00030	2.4	SD[45, 47-49]		

Pachyrrhynchus rufopunctatus (Waterhouse 1841)	OUNHM	No data	1841-1875	dull rose elytron scale	0.02149±0.00012 (3)	506.69	0.00211±0.00053	3.0	SD[45, 47-49]		
Pachyrrhynchus fimbriatus (Chevrolat 1841)	OUNHM	Manila, Philippines	23-Feb-1909	pale green elytron scale	0.02603 (1)	241.42	0.00867	0.7	*amorphous network[45, 47-49]		
Pachyrrhynchus forsteni (Vollhenhoeven 1864)	OUNHM		7-Feb-1909	bright white elytron scale	0.02079±0.00117 (2)	302.68	0.01160±0.00212	0.5	*amorphous network[45, 47-49]		
Apocyrtus aurora (Chevrolat 1881)	OUNHM	Mindanao, Philippines	No data	violet elytron scale	0.01976±0.00027 (3)	550.92	0.00257±0.00067	2.4	SD		
Tribe Phyllobiini											
Phyllobius sp.	CSIRO ANIC	Germany	June 1958	yellowish-green elytron scale	0.02511±0.00012 (6)	433.41	0.00168±0.00024	3.7	SD[37, 50, 51]	585.9 (150.0)	1.17 (0.3)
Tribe Polydrusini											
Polydrusus sp.	CSIRO ANIC	New Haven, CT, USA	May 1919	green elytron scale	0.02474±0.00031 (4)	440.02	0.00209±0.00035	3.0	SD[52]	545.8 (130.0)	1.07 (0.13)
[e]*Apodrosus stenoculus* (Girón and Franz 2010)	CSIRO ANIC	Dominican Republic	June 2008	blue elytron scale	0.02423 (1)	449.13	0.00360	1.7	SD		
[e]*Apodrosus viridium* (Girón and Franz 2010)	CSIRO ANIC	Dominican Republic	June 2008	green elytron scale	0.02295 (1)	474.15	0.00239	2.6	**Fddd*		
[e]*Apodrosus epipolevatus* (Girón and Franz 2010)	CSIRO ANIC	Puerto Rico, USA	Jan 2008	red elytron scale	0.01709 (1)	636.76	0.00263	2.4	SD		
[e]*Apodrosus wolcotti* (Marshall 1922)	CSIRO ANIC	Puerto Rico, USA	Dec 2006	brown elytron scale	0.01774 (1)	354.24	0.00469	1.3	*amorphous network		
Tribe Sitonini											
Sitona sp.	CSIRO ANIC	Tanunda, South Australia	May 1986	dull reddish elytron scale	0.02173±0.00064 (4)	496.82	0.00344±0.00090	1.8	SD	625.7 (412.2)	1.08 (0.14)
Sitona gressorius (Fabricius 1792)	OUNHM	No data	No data	pale red elytron scale	0.02079±0.00038 (2)	523.45	0.00250±0.00027	2.5	SD		

Catachaenus circulus (Eydoux et Soul 1839)	OUNHM	Manila, Phillipines	No data	blue-green elytron scale	0.02518±0.00012 (2)	352.91	0.00242±0.00021	2.6	SD		
Tribe Tanymecini											
Platyaspistes venustus (Erichson 1834)	YPM 707822	El Manzano, Chile	Nov 1951	green elytron scale	0.02647±0.00009 (5)	335.2	0.00146±0.00065	4.3	SG	564.1 (118.5)	1.19 (0.33)
Subtribe Tanymecina											
Pachnaeus opalus (Olivier 1807)	YPM 707825	Monroe County, Florida	Nov 1931	pale blue elytron scale	0.01634±0.00024 (6)	625.13	0.00214±0.00044	2.9	*SD(2) + SG		
Pachnaeus sp.	OUNHM	St. Domingo	No data	light green elytron scale	0.02453±0.00052 (3)	443.72	0.00142±0.00004	2.9	SD		
Subtribe Tainopthalmina											
Amomphus (*Aspidiotes*) *cottyi* (Lucas 1858)	OUNHM	No data	No data	emerald green elytron scale	0.02346±0.00049 (3)	464.07	0.00291±0.00039	2.2	SD		
Tribe Tropiphorini											
Catasarcus carbo (Pascoe 1870)	CSIRO ANIC	Western Australia	Dec 1988	yellow elytron scale	0.02444±0.00051 (5)	445.45	0.00236±0.00060	2.7	SD	598.5 (201.7)	1.16 (0.29)
[e]*Leptopius glaucus* (Pascoe 1882)	CSIRO ANIC	Bungendore, NSW, Australia	No data	green elytron scale	0.02441 (1)	445.91	0.00392	1.6	SD		
Spartecerus sp.	CSIRO ANIC	Bloemhof, South Africa	Nov 1983	dull reddish elytron scale	0.01919±0.00062 (4)	327.74	0.00678±0.00154	0.9	*amorphous network	690.3 (421.4)	1.05 (0.09)
Polycomus sp.	OUNHM	Brasil	presented 1911	pale green elytron scale	0.01905±0.00027 (3)	466.56	0.00182±0.00022	3.4	SG		
Subfamily Hyperinae											
Tribe Cepurini											
Chloropholus nigropunctatus (Gory 1834)	OUNHM	Madagascar	No data	green elytron scale	0.02464±0.00066 (4)	360.88	0.00177±0.00015	3.5	SG		
Tribe Hyperini											
Hypera diversipunctata (Schrank 1798)	purchased	No data	No data	reddish-brown	0.02083±0.00057 (2)	521.63	0.00268±0.00049	2.4	SD[53]		

				elytron scale							
Subfamily Lixinae											
Tribe Cleonini											
Leucochromus imperialis (Zoubkoff 1837)	OUNHM	Turcoman	No data	off-white elytron scale	0.02431 (1)	258.44	0.00614	1.0	amorphous network		
Family Cerambycidae (flat-faced longhorn beetles)											
gen. et sp. nov.	CSIRO ANIC	Western Australia	20-Jan-1984	silvery elytron scale	not structured						
Subfamily Cerambycinae											
Tribe Rosalini											
[f]*Rosalia alpina* (Audinet- Serville 1833)	OUNHM	Switzerland	No data	pale blue horn scale	0.03333 (1)	188.52	0.01042	0.6	*amorphous network		
Tribe Coptommatini											
Coptomma mirabilis (Fabricius 1775)	OUNHM	Malay	No data	pale bluish-white elytron scale	0.02682±0.00068 (3)	234.35	0.00596±0.00053	1.1	*amorphous network		
Subfamily Lamiinae											
Tribe Lamiini											
Anoplophora birmanica (Hüdepohl 1990)	purchased (male)	Thailand	Sep 2002	greenish-yellow elytron scale	0.02930±0.00168 (4)	304.05	0.00226±0.00077	2.8	BCC spheres[16, 45, 54]	583.6 (100.3)	1.36 (0.65)
Anoplophora zonatrix (Thomson 1878)	purchased (male)	Thailand	Apr 2002	pale blue elytron scale	0.03112±0.00069 (4)	201.89	0.00579±0.00097	1.1	quasi-ordered spheres[16, 45, 54]	497.1 (153.4)	1.23 (0.41)
Anoplophora zonatrix (Thomson 1878)	purchased (male)	Thailand	Apr 2002	pale blue elytron scale	0.02939±0.00038 (2)	302.38	0.00538±0.00221	1.2	*BCC spheres[16, 45, 54]		
Anoplophora versteegi (Ritsema 1881)	purchased	Thailand	May 2002	pale blue elytron scale	0.01762±0.00063 (8)	356.64	0.00511±0.00055	1.2	quasi-ordered spheres[16, 45, 54]		
Anoplophora graafi	SI-USNM	Sumatra	No data	bluish-green	0.03065±0.00066 (11)	205.03	0.00468±0.00046	1.3	*quasi-ordered +	530.5 (127.2)	1.29 (0.52)

(Ritsema 1880)				elytron scale					FCC opal(5)[16, 45, 54]		
Anoplophora stanleyana (Hope 1840)	OUNHM	No data	No data	pale blue-green elytron scale	0.02920±0.00086 (4)	304.54	0.00461±0.00100	1.4	BCC spheres[16, 45, 54]		
Tribe Saperdini											
Glenea fortunei (Saunders 1853)	OUNHM	China	presented 1880	pale green elytron scale	0.02696±0.00037 (4)	233.07	0.00527±0.00047	1.2	*quasi-ordered spheres[45]		
Saperda cretata (Newman 1838)	YPM 706541	Worcester, MA	28-Jun-1908	pale white elytron scale					not structured		
Tribe Tmesisternini											
[f]*Tmesisternus* sp.	OUNHM	Moluccas	No data	bluish-white elytron scale	0.02540 (1)	247.33	0.01273	0.5	*amorphous network[18, 55]		
Tribe Tragocephalini											
Phosphorus jansoni (Chevorat 1861)	YPM 708913	Nigeria-Aredi	14-Aug-1959	yellow elytron scale	0.01701±0.00030 (4)	522.42	0.00258±0.00015	2.4	BCC spheres[56]		
Tribe Sternotomini											
Sternotomis c. callais (Fairmaire 1891)	YPM 707577	Congo	Apr 1980	bluish-green elytron scale	0.02857±0.00061 (3)	219.99	0.00329±0.00051	1.9	SP	539.6 (96.7)	1.23 (0.40)
Sternotomis pulchra bifasciata (Drury 1773)	YPM 707578	Nigeria, Western State	12-Dec-1911	green elytron scale	0.02830±0.00015 (7)	222.04	0.00308±0.00059	2.0	SP	550.4 (93.3)	1.24 (0.43)
Sternotomis pulchra bifasciata (Drury 1773)	YPM 707578	Nigeria, Western State	12-Dec-1911	red-brown elytron scale	0.02034±0.00050 (6)	308.96	0.00358±0.00055	1.8	amorphous network	774.1 (244.4)	1.25 (0.45)
Sternotomis mirabilis (Drury 1773)	YPM	Nimba cty, Liberia	7-Nov-1982	green elytron scale	0.02783±0.00018 (4)	225.76	0.00249±0.00049	2.5	SP	555.4 (97.9)	1.23 (0.41)
Sternotomis bohemani (Chevrolat 1844)	YPM 707583	Nigeria	6-Mar-1972	greenish-yellow elytron scale	0.02494±0.00014 (3)	251.89	0.00371±0.00020	1.7	*amorphous SP network	583.4 (193.0)	1.16 (0.28)
Freadelpha (*Sternotomis*) *murrayi* (Chevrolat 1855)	OUNHM	Old Caledonia	1855	greenish-white elytron scale	0.01694±0.00011 (3)	370.97	0.00258±0.00024	2.4	*amorphous SP network		
Tribe Prosopocerini											

Prosopocera lactator meridionalis (Jordan 1903)	SI-UNSM 213112	No data	10-May-1905	pale greenish-white elytron scale	0.01725±0.00048 (4)	515.38	0.00379±0.00266	1.7	BCC sphere network[15, 49]		
Anoplasthala (*Prosopocera*) *lactator* (Fabricius 1801)	OUNHM	Guinea	Jun 1908	pale bluish-green elytron scale	0.01721±0.00068 (3)	516.82	0.00289±0.00063	2.2	BCC sphere network[15, 49]		
Order Hymenoptera											
Family Apidae (bees)											
Subfamily Apinae											
Tribe Anthophorini											
Amegilla cingulata (Fabricius 1775)	CSIRO ANIC	N. Queensland, Australia	1-9 Jun 1971	bluish-green setae	0.02977±0.00047 (5)	243.69	0.00372±0.00062	1.7	inverse 2D hexagonal columnar[23]	544.3 (129.5)	1.29 (0.52)
Tribe Melectini											
Thyreus pictus (Smith 1854)	YPM 707799	Monianku, Kenya	19-Mar-1974	turquoise blue setae	0.03171±0.00041 (8)	198.14	0.00809±0.00052	0.8	sponge (amorphous network)	525.7 (149.2)	1.33 (0.58)
Thyreus nitidulus (Fabricius 1804)	CSIRO ANIC	No data	2-Jul-1991	iridescent blue setae	0.03285±0.00024 (5)	191.29	0.00695±0.00035	0.9	inverse 2D twisted columnar	507.4 (96.7)	1.33 (0.58)
Order Diptera											
Suborder Brachycera											
Infraorder Asilomorpha											
Superfamily Asiloidea											
Family Bombyliidae											
Subfamily Anthracinae											
Tribe Exoprosopini											

Exoprosopa sp.	OUNHM	Ceylon	No data	silvery setae					not structured

Class Arachnida

Order Araneae

Suborder Araneomorphae

Family Salticidae (jumping spiders)

Saitis (*Attus*) *splendidus* (Walckenaer 1837)	OUNHM	No data	No data	white thorax scale					not structured[57-60]
gen. et sp. nov.	OUNHM	No data	No data	blue abdomen scale	0.04677±0.00040 (3)	155.12	0.00569±0.00101	1.1	inverse 2D hexagonal columnar[57-60]

Suborder Mygalomorphae

Family Theraphosidae (tarantulas)

Subfamily Poecilotheriinae

Poecilotheria metallica (Pocock 1899)	OUNHM Ray Gabriel Collection 2007-064	No data	30-May-2007	bluish-purple leg setae (male)	0.04448±0.00098 (4)	143.31	0.00815±0.00080	0.8	*perforated lamellar[24, 25]

Subfamily Ornithoctoninae

Haplopelma lividum (Smith 1996)	OUNHM Ray Gabriel Collection 2007-064	pet trade	No data	blue leg setae	0.04141±0.00093 (4)	151.76	0.01902±0.01554	0.3	*perforated lamellar[24, 25]
Cyriopagopus schioedtei (Thorell 1891)	OUNHM Ray Gabriel Collection 2009-064	No data	2008	yellowish-green leg setae (male)					not structured[24, 25]

Subfamily Aviculariinae

Ephebopus cyanognathus (West et	OUNHM Ray Gabriel	pet trade	No data	bluish-purple chelicerae	0.04510±0.00027 (2)	139.32	0.01096±0.00190	0.6	*perforated lamellar[24, 25]

Marshall 2000)	Collection 2007-064	setae (male)

[a] Mean lattice parameters estimated from the slope of the plots of the moduli of assigned *hkl* Miller indices of Bragg peaks versus the corresponding reciprocal lattice spacings; For quasi-ordered or amorphous systems, $2\pi / q_{pk}$ gives the peak spatial periodicity or the structural correlation length

[b] Optical coherence length is calculated from the full widths at half-maximum (FWHM) of pseudo-Voigt fits to the first-order SAXS peaks, $\xi = 2\pi / \Delta q_{pk}$

[c] SD – single diamond (*Fd*-3*m*); SG – single gyroid ($I4_132$); *Fddd* – face-centred orthorhombic; SP – primitive/simple cubic (*Pm*-3*m*); BCC – body-centred cubic (*Im*-3*m*); FCC – face-centred cubic (*Fm*-3*m*). Numbers within parentheses indicate number of assays from scales with the corresponding nanostructure. Numbers in superscript list published references on structural colors in this genus/family, for comparison

[d] Effective or average refractive index (n_{avg}) estimated using Bragg's Law (Main text Eq. 1) and the chitin filling fraction (ϕ) within parentheses estimated using Maxwell-Garnett effective medium approximation theory[61]

[e] The SAXS data from these 7 scales were obtained by AES at the Australian Synchrotron

[f] The SAXS data from these 3 scales were obtained at the Diamond Light Source

*Tentative nanostructural diagnoses